

Optimal Falling Track Design for Twice-detonating Fuze of Double-event Fuel-air Explosive with High Speed

Congliang Ye and Qi Zhang*

State Key Laboratory of Explosion Science and Technology, Beijing Institute of Technology, Beijing - 100 081, China

*E-mail: qzhang@bit.edu.cn

ABSTRACT

To prevent the initiation failure caused by the uncontrolled fuze and improve the weapon reliability in the high-speed double-event fuel-air explosive (DEFAE) application, it is necessary to study the TDF motion trajectory and set up a twice-detonating fuze (TDF) design system. Hence, a novel approach of realising the fixed single-point center initiation by TDF within the fuel air cloud is proposed. Accordingly, a computational model for the TDF motion state with the nonlinear mechanics analysis is built due to the expensive and difficult full-scale experiment. Moreover, the TDF guidance design system is programmed using MATLAB with the equations of mechanical equilibrium. In addition, by this system, influences of various input parameters on the TDF motion trajectory are studied in detail singly. Conclusively, the result of a certain TDF example indicates that this paper provides an economical idea for the TDF design, and the developed graphical user interface of high-efficiency for the weapon designers to facilitate the high-speed DEFAE missile development.

Keywords: Double-event fuel-air explosive; Twice-detonating fuze; Initiation; Motion trajectory; MATLAB; Graphical user interface

1. INTRODUCTION

Nowadays the warhead is designed from the conventional chemical explosive charge to the fuel-air explosive (FAE) which can cover larger area with no inhibition by land contour or protective structures in military applications¹. FAE weapons have been equipped, or are being developed and improved in many countries. A double-event fuel-air explosive (DEFAE) warhead mainly consists of the mixed fuel, a fuze, a shell, a central pipe and a high-explosive (HE) charged in the central pipe. The mixed fuel is filled in a column structure and dispersed by the center explosion drive. The dispersed fuel mixing with air forms the explosive fuel air cloud. Then mixture cloud will detonate by the initiation of the twice-detonating fuze (TDF). Meanwhile, high-speed missiles are becoming a new research hotspot for its tactical mobility and momentum. Furthermore, the high-speed DEFAE has a better application prospect in the real warfare. However, the high speed may induce TDF to fly out of the fuel/air cloud, which increases the difficulty of the initiation by TDF. Hence, it is necessary to study the TDF motion state and set up a TDF design system, so as to prevent the initiation failure caused by uncontrolled TDF and enhance the weapon system reliability in the high-speed DEFAE application.

At present, much work on FAE development has been completed numerically and experimentally. Important features of fuel air explosives studies on different performance parameters, namely, minimum initiation energy, fuel droplet

size, sensitivity to detonation etc. and current trends in this field of research have been briefly discussed by Rao². Singh³, *et al.* developed a theoretical model for the prediction of the mean-mass diameter of droplets produced by the fragmentation of liquid fuel in the near field and a distribution model for the initial distribution of the droplet diameter in a FAE device. Zhang⁴, *et al.* studied the critical ignition temperature of FAE with the charge of solid-liquid mixed fuel and the fuel motion state in the acceleration process⁵, and later revealed the dispersal character of the mixed fuel by the burst HE charged in the central pipe⁶. Singh⁷, *et al.* developed the design of a diode laser proximity sensor based on the principle of optical triangulation for FAE bomb applications. Apparao⁸, *et al.* studied the formation of the unconfined detonable vapor cloud by explosive ways. Simultaneously, With the Tri-nitro Toluene (TNT) equivalence method, Apparao⁹, *et al.* analysed the blast parameters of the unconfined aerosols of 4.2 kg PO formed by breaking open the cylindrical canister with the help of axially positioned central burster charge. Liu compared the detonation characteristics in energy output of gaseous JP-10 and propylene oxide in air by CFD simulations¹⁰.

As we have seen, the previous available publications mainly focus on the fuel dispersal, aerosol cloud sizes, fuel density distribution and evaluation of the detonation power. However, few papers center on the secondary initiation by TDF, especially the TDF motion trajectory at the high dynamics. At present, the TDF initiation has 2 modes, viz., random initiation and high energy initiation at a fixed point^{11,12}. In the case of random initiation, there are lots of drawbacks

such as high random motion state, small amount of central HE, low reliability of detonation, unexpected burning and deflagration^{13,14}. Thus, to avoid TDF being ejected outside of cloud^{15,16}, the second mode is selected. Moreover the shock wave overpressure based on FAE explosion would decrease with the increase of the number of secondary initiation points. The overpressure reduced by 48%~52% from a single point to four points¹⁷. As a result, the single-point initiation mode is adopted for generating the greatest shock wave overpressure. Ultimately, with unifying the two modes above, a new approach of fixed single-point initiation by high energy is proposed.

The successful TDF initiation, one of the key technical problems, is the precondition that DEFAE can unleash its enormous detonation power. As full-scale experimental investigations are extremely expensive and difficult, simulation research approaches based on modelling are of great significance. Consequently in the present study, for purpose of any new DEFAE development, to eliminate the initiation failure hazard, three major issues have been figured out. Firstly, the TDF motion state with the nonlinear mechanics analysis was modeled. Moreover, the TDF guidance design system was programmed using MATLAB with the equations of mechanical equilibrium. The graphical user interface (GUI) was designed, which is used easily to provide guidance for DEFAE weapon designers with various input parameters. In addition, influences of various input parameters on the TDF motion trajectory were studied in detail singly. Subsequently, a certain TDF example was designed to provide an optimisation design idea.

2. COMPUTATIONAL MODEL

The physical model likes that, TDF tied with parachute is embedded in the top of DEFAE warhead, which is right above the central burst high-explosive (HE) pipe, shown in Fig. 1. The working principle of DEFAE warhead is as follows. Once the high speed DEFAE warhead detects the objective, the central HE detonates to drive fuel to spread and mix with air. At the same time, TDF is activated by the output signal. With the restraint of parachute, TDF falls inside the cloud along with the original trajectory. By using millisecond delay initiation of TDF, the fuel-air cloud

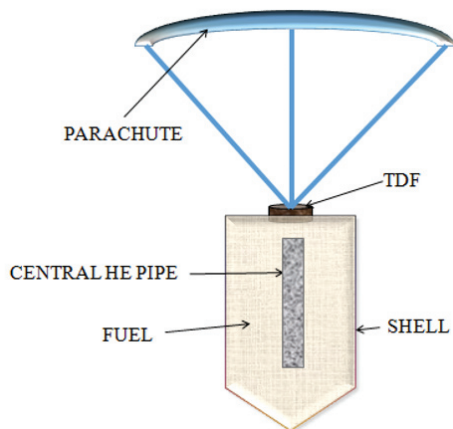


Figure 1. Sketch of the DEFAE warhead with the fixed single-point initiation TDF.

detonates when TDF reaches a predetermined position. Based on the above principle, it is known that the warhead falls down under the action of the self-gravity, the tension of parachute lines and the aerodynamic drag. Moreover when the center HE explodes, the TDF motion is also affected by center HE explosion force.

For the computational mode, it is assumed the TDF and parachute always fall down on a vertical plane after the central HE initiation. The TDF is supposed as a mass point without the plastic deformation in the rigid motion. A coordinate axis in which the positive direction is straight downwards is set up. The origin of coordinates is the right place of TDF just in time of the center HE initiation. At this point, $t = 0$, $v = v_0$. To emphasis on analysing the TDF falling track after the central HE explosion, the TDF motion is a two-stage process including the rapid deceleration phase and the free falling phase.

2.1 Force Analysis

At the rapid deceleration phase, taking the TDF as the research object, the TDF motion state is affected by TDF self-gravity (G_y), parachute ropes tension (R_1), central HE explosion pressure (R_p), aerodynamic drag (R_a). Taking the parachute as the research object, its motion is influenced by parachute self-gravity (G_s), parachute rope tension, parachute drag (R_s), shown in Fig. 2(a). At the free falling phase, the center HE explosion doesn't exert pressure on TDF anymore. This means the pressure is nonexistent, the rest are the same as the rapid deceleration phase, shown in Fig. 2(b). The three forces, viz., parachute ropes tension, central HE explosion pressure and aerodynamic drag play important roles in the TDF deceleration. The detailed presentations of some crucial

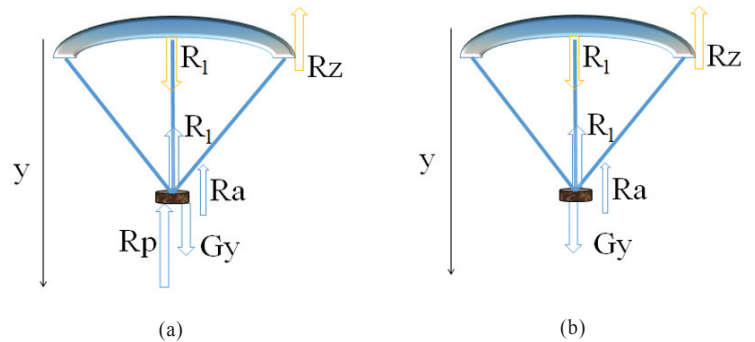


Figure 2. TDF and parachute force analysis of (a) rapid deceleration phase and (b) free falling phase. forces are clarified separately in particular.

2.1.1 Parachute Drag

The parachute drag is made up of the quasi-steady fluid aerodynamic drag and the inertia resistance¹⁸, so its expression is

$$R_z = R_s + R_f \quad (1)$$

where R represents the force, R_z is the parachute drag; R_s is the quasi-steady fluid aerodynamic drag; R_f is the inertia resistance of parachute.

According with the aerodynamics¹⁹, R_s is expressed by

$$R_s = \frac{1}{2} \rho A_s C_s \left(\frac{dy}{dt} \right)^2 \quad (2)$$

where ρ is the gas density near the parachute, A_s is the vertical projection area of the fully inflated parachute; C_s is the air drag coefficient of parachute relative to the characteristic area which is just A_s . Here is known that C_s changes with the shape of the parachute. But after the full inflation of the parachute, the vertical projection area of the parachute is constant. This means A_s is constant and C_s tends to a stable value. As for the parachute with the fixed material and size, an empirical value is taken, $C_s = 1.4$ ²⁰.

The gas density near the parachute is changeable. But before the parachute falls into the fuel/air cloud, it changes with the altitude, but almost slightly, which is negligible. After the parachute and TDF fell into the cloud, its value increases mainly due to the influence of fuel/air density. However, based on the CFD numerical simulations of fuel dispersal and experimental results, the fuel concentration in the cloud is not evenly distributed, so we can only use a mean estimate method, the change of fuel concentration is about 0.01-0.2 kg/m³, or even smaller, only a pretty small local area has a high density in quite short time. Compared with the atmospheric density of 1.293 kg/m³, the change range is small. Therefore, to facilitate programming and modelling, a constant value approximate to the atmospheric density is taken in next simulations.

R_f can be expressed in the momentum form. R_f is equal to the force which makes the added mass accelerate. According with the Newton second law, its expression is

$$R_f = m_f \frac{dv}{dt} = m_f \frac{d^2 y}{dt^2} \quad (3)$$

where m_f is the added mass of the parachute.

The inertia resistance is the added motion resistance due to overcoming the mass inertia in the unsteady motion, like adding a new mass in the motion object. The real mass doesn't increase, so it is also called false mass which is related to the character and structure of the motion object²¹. The theoretical calculation of the added mass of the parachute is a complex issue which has not been solved completely. Therefore the empirical algorithm is used in the engineering. Here the sphere empirical method is adopted, which is close to the true circumstance of the fully inflated parachute. In this way, the added mass is approximate to the air mass in a sphere. The radius of this sphere is the same as the radius of A_s . So the added mass is expressed by

$$m_f = \frac{4}{3} \rho \pi r^3 \quad (4)$$

where r is the radius of A_s . Here, the surface area of fully inflated parachute (S) is approximately twice of A_s . So the vertical projection area of the fully open parachute is expressed by

$$A_s = \pi r^2 = \frac{1}{2} S \quad (5)$$

With Eqns. (4) and (5), the added mass becomes

$$m_f = \frac{4}{3} \rho \pi \left(\frac{S}{2\pi} \right)^{\frac{3}{2}} = \frac{1}{3} \left(\frac{2}{\pi} \right)^{\frac{1}{2}} \rho S^{\frac{3}{2}} \quad (6)$$

Seen from Eqn. (6), the added mass can be expressed by S . This means the inertia resistance can be controlled by changing the parachute superficial area. In the Eqn. (4), r is invariable after the full inflation of the parachute; the added mass will not vary with time, which can be written by $\frac{dm_f}{dt} = 0$.

2.1.2 Pressure of Central HE Explosion on TDF

From the previous research results, seem from the Fig. 3, there is a sharp jump in the air explosion shock wave pressure and then the overpressure drops rapidly and almost linearly. As the TDF bottom is in succession with the top of the central HE pipe, which means there is no propagation distance of the shock wave, here is assumed that the central HE detonates instantly and fully converts to the high-pressure detonation gas when t is 0 s. This means it is the maximum blast overpressure (a) acting on TDF when $t = 0$ s. In addition, due to the high falling speed of TDF, the overpressure decays relatively faster. When the overpressure decays to 0, the central explosion acting force disappears. Thus, the previous stage of overpressure propagation and growth and the oscillation stage are basically ignored, and the following approximate linear equation of overpressure attenuation is used in our modelling. Accordingly, the central HE explosion continues to be exerted on TDF in a very short time (b).

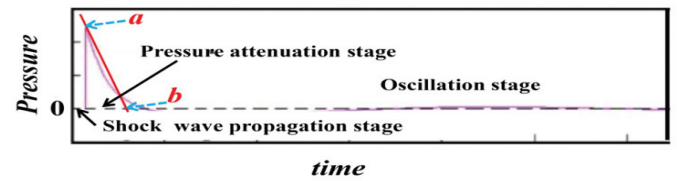


Figure 3. Typical waveform structure of the air explosion shock wave²².

Based on the analysis above, here is an assumption for the central explosion pressure acting on TDF: the pressure of the central explosion gas vertically acts on the TDF bottom and the intensity of the pressure has a significant linear correlation with time and its initial load. So the expressions of the pressure and its intensity are, respectively.

$$R_p = A_y P(t) \quad (7)$$

$$P(t) = -\frac{a \times 10^6}{b \times 10^{-3}} \cdot t + a \times 10^6 \quad (8)$$

where R_p is the central HE explosion pressure on the TDF; $P(t)$ is the intensity of R_p ; A_y is the TDF base area; a is the initial load of the central HE explosion, which is the maximum blast pressure from central explosion; b is the duration of the central HE explosion acting on TDF.

2.1.3 Aerodynamic Drag of TDF

The aerodynamic drag of the TDF:

$$R_a = \frac{1}{2} \rho A_y C_y \left(\frac{dy}{dt} \right)^2 \quad (9)$$

where R_a is the aerodynamic drag of the TDF; A_y is the

characteristic area of the TDF; C_y is the aerodynamic drag factor of the TDF.

The TDF size is much smaller than the parachute size. There are several orders of magnitude in their characteristic area. Meanwhile C_s is also greater than C_y . The ratio of their drag characteristics approaches 0, viz., $(CA)_y / (CA)_s = 0$. This indicates R_a has the far less influence on the TDF deceleration motion than R_s . Therefore R_a is negligible.

2.2 TDF Motion State Equations

2.2.1 TDF Motion State Equation at Rapid Deceleration Phase

In the coordinate system of a vertical plane, setting up the kinetic equations of the parachute and the TDF respectively as follows:

$$\frac{d^2 y}{dt^2} m_s = m_s g + R_l - R_z \quad (10)$$

$$\frac{d^2 y}{dt^2} m_y = m_y g - R_l - R_p - R_a \quad (11)$$

By addition of Eqns. (11) and (10), the kinetic equations of the TDF and the parachute become one:

$$(m_y + m_s) \frac{d^2 y}{dt^2} = (m_y + m_s) g - R_p - R_a - R_z \quad (12)$$

Because R_a is negligible, substituting Eqns. (1), (2), (3), (7), (8) into Eqn. (12) in the meanwhile, the new equation is

$$(m_y + m_s) \frac{d^2 y}{dt^2} = (m_y + m_s) g - A_y \left(-\frac{a \times 10^6}{b \times 10^{-3}} \cdot t + a \times 10^6 \right) - m_f \frac{d^2 y}{dt^2} - \frac{1}{2} \rho A_s C_s \left(\frac{dy}{dt} \right)^2 \quad (13)$$

Rearranging the Eqn. (13),

$$(m_y + m_s + m_f) \frac{d^2 y}{dt^2} = -\frac{1}{2} \rho A_s C_s \left(\frac{dy}{dt} \right)^2 + \frac{a A_y}{b} \times 10^9 \cdot t - a A_y \times 10^6 + (m_y + m_s) g \quad (14)$$

$$\begin{aligned} \frac{d^2 y}{dt^2} = & -\frac{\rho A_s C_s}{2(m_y + m_s + m_f)} \left(\frac{dy}{dt} \right)^2 \\ & + \frac{a A_y}{b(m_y + m_s + m_f)} \times 10^9 \cdot t \\ & - \frac{a A_y}{(m_y + m_s + m_f)} \times 10^6 \\ & + \frac{m_y + m_s}{(m_y + m_s + m_f)} g \end{aligned} \quad (15)$$

Abbreviating the Eqn. (15), the TDF motion state equation at the rapid deceleration phase is developed as

$$\frac{d^2 y}{dt^2} = -k_1 \left(\frac{dy}{dt} \right)^2 + k_2 \cdot t - k_3 + k_4 g \quad (16)$$

where

$$\begin{aligned} k_1 &= \frac{\rho A_s C_s}{2(m_y + m_s + m_f)} \\ k_2 &= \frac{a A_y}{b(m_y + m_s + m_f)} \times 10^9 \\ k_3 &= \frac{a A_y}{(m_y + m_s + m_f)} \times 10^6 \\ k_4 &= \frac{m_y + m_s}{m_y + m_f} \\ A_s &= \frac{1}{2} S \\ m_f &= \frac{1}{3} \left(\frac{2}{\pi} \right)^{\frac{1}{2}} \rho S^{\frac{3}{2}} \end{aligned}$$

2.2.2 TDF Motion State Equation at Free Falling Phase

R_p is nonexistent at this phase, the rest are the same as the rapid deceleration phase. In fact, the motion state equation of the TDF is the Eqn. (12) just without R_p which is as follow:

$$\frac{d^2 y}{dt^2} = -k_1 \left(\frac{dy}{dt} \right)^2 + k_4 g \quad (17)$$

2.2.3 Coupled Motion State Equations of High Speed TDF during Entire Falling Process after Central HE Explosion

$$\left\{ \begin{aligned} \frac{d^2 y}{dt^2} &= -k_1 \left(\frac{dy}{dt} \right)^2 + k_2 t - k_3 + k_4 g, 0 \leq t < bms \\ \frac{d^2 y}{dt^2} &= -k_1 \left(\frac{dy}{dt} \right)^2 + k_4 g, t \geq bms \\ A_s &= \frac{1}{2} S \\ m_f &= \frac{1}{3} \left(\frac{2}{\pi} \right)^{\frac{1}{2}} \rho S^{\frac{3}{2}} \\ k_1 &= \frac{\rho A_s C_s}{2(m_y + m_s + m_f)} \\ k_2 &= \frac{a A_y}{b(m_y + m_s + m_f)} \times 10^9 \\ k_3 &= \frac{a A_y}{(m_y + m_s + m_f)} \times 10^6 \\ k_4 &= \frac{m_y + m_s}{m_y + m_f} \end{aligned} \right.$$

The above simultaneous equations describe accurately the whole falling slowdown track of the high speed TDF from this time of the center HE initiation to when the TDF detonates the

fuel-air cloud. The complicated equations cannot be directly solved for the analytic solution. Accordingly the MATLAB software is utilised to program the equation group for the numerical solutions and figures of the TDF displacements in various conditions.

2.3 Validation of Numerical Model

To prove the validity of this numerical model above, the drop test²³ of cruciform parachute at its steady drop stage is compared with the simulation result, as shown in Fig. 4, which shows that the numerical result is in good agreement with the experimental results, the error between them is less than 8.2%. As a result, the numerical model has a good reliability. The main design parameters of cruciform parachute are exhibited in Table 1.

Table 1. Main parameters of parachute in drop test

| Parachute mass/kg | Parachute area/m ² | Load mass/kg | Drag coefficient | Initial velocity/(m/s) |
|-------------------|-------------------------------|--------------|------------------|------------------------|
| 5 | 87 | 231 | 1.4 | 11.5 |

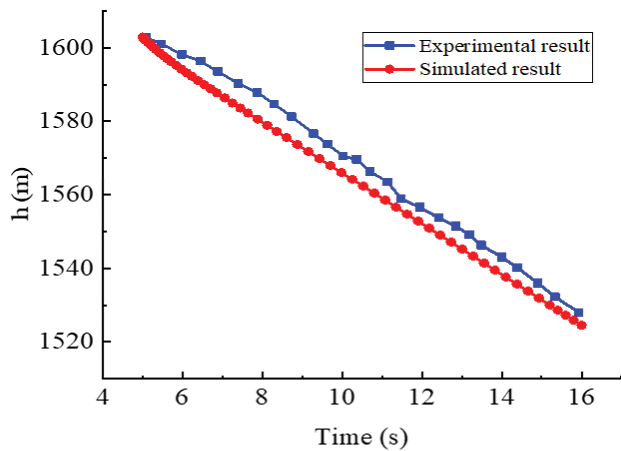


Figure 4. Altitude history of parachute-object system versus time in experiment and simulation.

2.4 Graphical User Interface Design

The graphical user interface is the human-computer interaction intermediary with powerful functions, can complete many complex program modules²⁴.

A digital parameters setting system based on LCD display and keyboard input is provided in the MATLAB. Taking the reference group of parameters as an instance, the English visual input interface version is illustrated in Fig. 5.

By clicking on the ‘Run’ button, a subsidiary interface is displayed in Fig. 6. The Users can also select the Save, Print, Zoom in, Zoom out, Pan and other functions through the menu bar to save the data graphics and the like. Subsequently it only needs to click the ‘Exit’ button of the parameter setting interface to close the simulation.

3. RESULTS

Setting a reference group of parameters for the TDF motion: $a = 1$ MPa, $b = 50$ ms, $A_y = 0.01$ m², $m_y = 2$ kg, $m_s = 1$ kg, $S = 1.5$ m², $C_s = 1.4$, $v_0 = 200$ m/s, the falling TDF track is

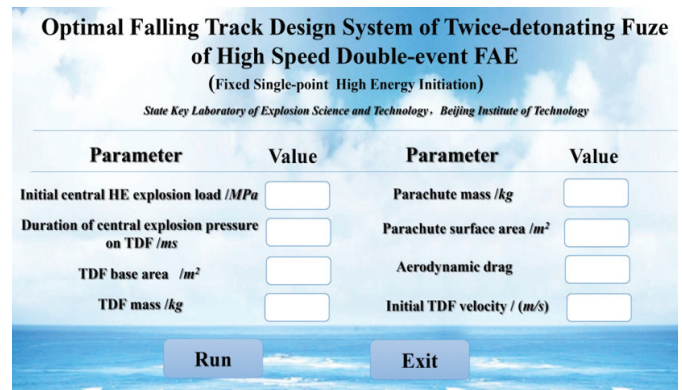


Figure 5. Graphical user interface of input parameters.

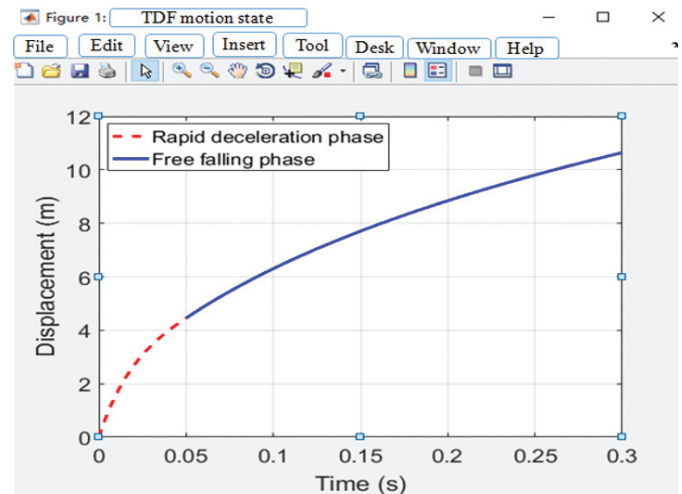


Figure 6. Output pattern of GUI simulation.

represented in Fig. 7(a). Limited by the length of the article, then only five selected key factors are to be studied next. Nonetheless, the other three factors are essential to the TDF motion state.

4. DISCUSSIONS

4.1 Analysis on Various Parameters

4.1.1 Impact of v_0 on TDF Displacement

Under the condition of other technological parameters unchanged, taking v_0 as 200 m/s, 400 m/s and 600 m/s, respectively, the results are displayed in Fig. 7(b). Seen from Fig. 7(b), in the same amount of time, the falling distance of the TDF would increase with the increase of the initial falling velocities of the TDF at the time of the central HE initiation.

4.1.2 Impact of m_y on TDF Displacement

The TDF mass correlated with its structure determines whether the fuel-air cloud detonates successfully by the high energy or not. It also has a strong tie to the destruction efficiency of the DEFAE. Thus it is extremely necessary to conduct the research on the factor of m_y . Unchanging the other technological parameters and taking m_y as 2 kg, 4 kg, and 6 kg, respectively, the results are displayed in Fig. 7(c). Seen from Fig. 7(c), in the same amount of time, the falling distance of the TDF would increase with the increase of the TDF mass.

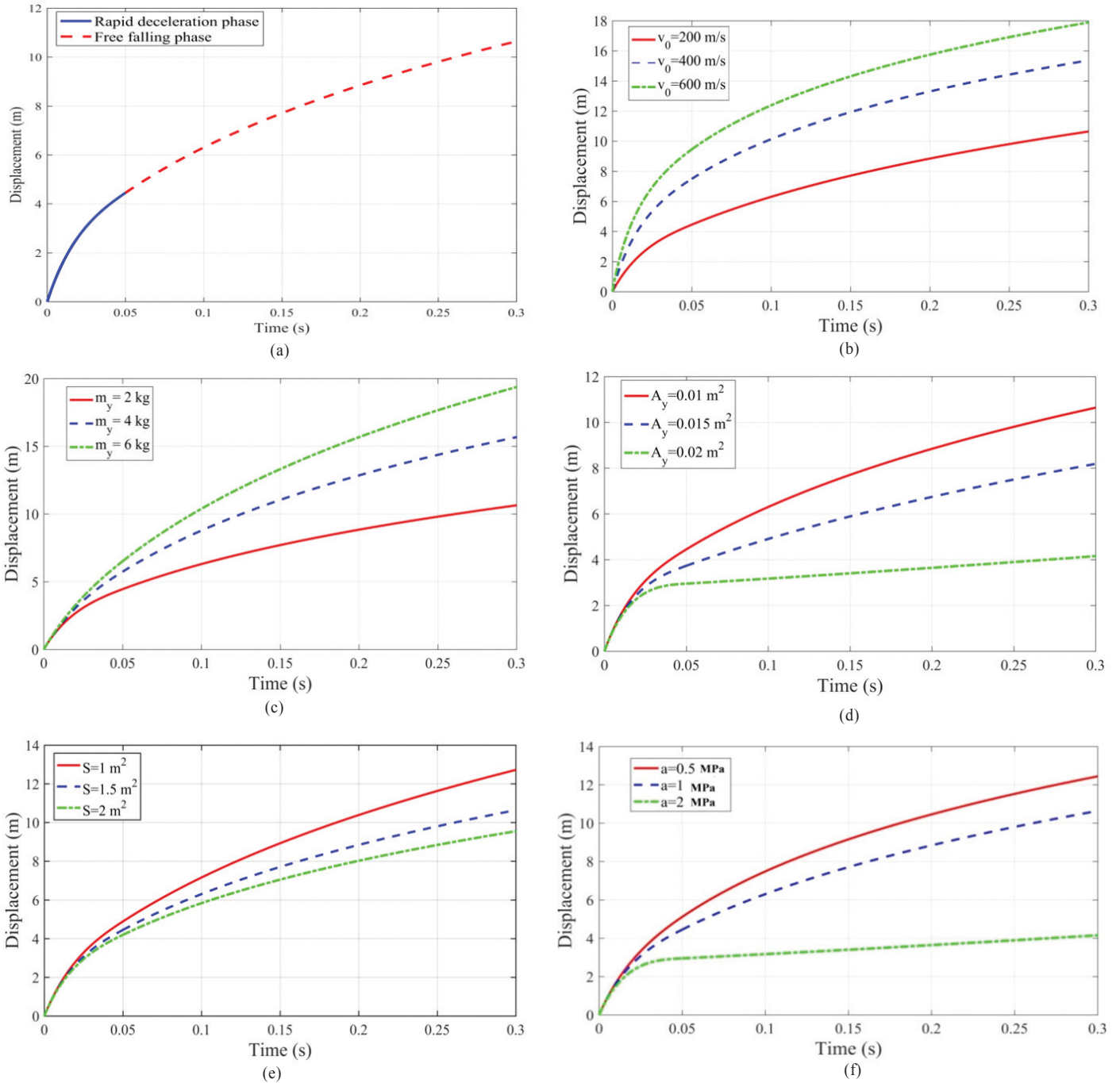


Figure 7. (a) Falling track of the TDF as a reference. Comparison of the TDF tracks affected by various, (b) Initial falling velocities, (c) TDF mass, (d) TDF base areas, (e) Parachute surface areas and (f) Initial central HE explosion loads.

4.1.3 Impact of A_y on TDF Displacement

It is that the center HE explosion acting on the TDF bottom so that the TDF could be slow down instantaneously. The TDF base area is also highly relevant to its mass and structure. Thus it is needed to study on the factor of A_y . Under the condition of other parameters unchanged, taking as 0.01m^2 , 0.015m^2 , 0.02m^2 , respectively, the results are displayed in Fig. 7(d). Seen from Fig. 7(d), in the same amount of time, the TDF displacement would decrease with the increase of the base area of the TDF. The central HE explosion pressure on the TDF is proportional to the TDF base area. Known from another

perspective, viz., by the Eqn. (7), the greater the action surface on the TDF results into the greater the pressure exerted by the central HE explosion on the TDF.

4.1.4 Impact of S on TDF Displacement

The superficial area of the parachute links with its cost. Therefore, in such circumstance of satisfying other DEFAE design objections, it is economical to keep the parachute as small as possible. Under the condition of other parameters unchanged, taking S as 1m^2 , 1.5m^2 , 2m^2 , respectively, the results are displayed in Fig. 7(e). Seen from Fig. 7(e), in the

same amount of time, the falling distance of the TDF would decrease with the increase of the superficial area of the parachute. Thus if the TDF falling displacement and other factors unchanged are given, the minimum S could be sought step by step.

4.1.5 Impact of a on TDF Displacement

The central HE explosion exerts a transient but tremendous impact on the falling TDF so that TDF reduces the falling speed rapidly. By the Eqns. (7) and (8), the initial central HE explosion pressure load and the pressure duration are crucial to the TDF deceleration. Under the condition of other parameters unchanged, taking a as 0.5 MPa, 1 MPa, 2 MPa, respectively, the results are displayed in Fig. 7(f). Seen from Fig. 7(f), in the same amount of time, the falling distance of the TDF would decrease with the increase of the initial load of the center HE explosion. In the case of taking a as 2 MPa, the falling distance is very small at the free falling phase, which means a can direct effectively the TDF to the preset region.

4.2 Ensamble for Optimisation Design of TDF

Here, it is a hypothesis that a new type of 500 kg DEFAE missile with a sonic attack speed of 360 m/s is needed to be developed. The center of the fuel/air cloud formed after the central explosion moves down 15 m in 300 ms. Therefore, in order to make the cloud field coupled with the TDF under such conditions, it is necessary to make TDF fall about 15m at 300ms, which is just able to implement the fixed initiation by high energy. Whereupon, the programmed GUI is employed to continuously adjust other controllable parameters, so as to optimise the TDF design to meet the displacement at 300 ms. For a specific missile, it is supposed that the central HE and parachute are invariable, where, $a = 100$ MPa, $b = 10$ ms, $S = 2$ m², $A_y = 0.005$ m², $m_s = 5$ kg, $C_s = 1.4$. Thus, with attempts of various TDF masses, it is found that when $m_y = 4.225$ kg, the TDF can get to the 15.03 m at 300 ms along the axis within the fuel/air cloud, as shown in Fig. 8. In the similar way, the relationships of other parameters versus the TDF motion trajectory can be acquired, so as to optimise the whole DEFAE weapon design.

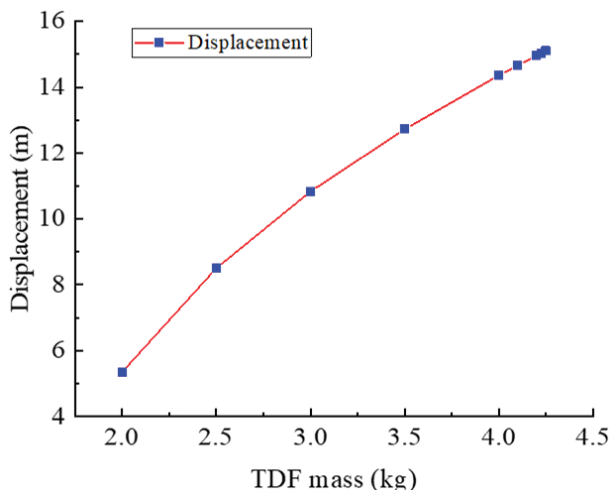


Figure 8. Curve of TDF displacement versus TDF mass.

5. CONCLUSIONS

To avoid the TDF flying out of fuel/air cloud and prevent the initiation failure, an original fixed single-point initiation solution is presented. Therewith, the TDF motion trajectory is modelled with the nonlinear mechanics analysis, and the numerical model is verified by a drop test. Accordingly, the GUI for the TDF design system is developed using MATLAB.

Furthermore, by using this GUI, the simulation results indicate that the TDF displacement would increase with the increase of the initial falling velocity and TDF mass. On the contrary, the falling distance would reduce with the increase of the initial central explosion load, TDF bottom area and parachute surface area.

Ultimately, by the similar design approach of the ensamble of 500 kg DEFAE missile with a sonic attack speed of 360m/s, the relationships of the design parameters versus the TDF motion trajectory can be acquired, so as to optimise any DEFAE missile development.

REFERENCES

- Luo, A.M. & Zhang, Q. Numerical simulation of temperature effects on warhead explosion products. *Chinese J. High Pre. Phys.*, 2006, **30** (1), 45-50. doi: 10.1016/j.mineng.2005.09.006.
- Rao AA. Fuel air explosives. *Def. Sci. J.*, 2014, **1**, 23-28. doi: 10.14429/dsj.37.5888
- Singh, S.K. & Singh, V.P. Extended near-field modelling and droplet size distribution for fuel-air explosive warhead. *Def. Sci. J.*, 2001, **51** (3), 303-314. doi: 10.14429/dsj.51.2244.
- Zhang, Q.; Bai, C.H.; Dang, H.Y. & Yan, H. Critical ignition temperature of fuel-air explosive. *Def. Sci. J.*, 2004, **54**, 469-474. doi: 10.14429/dsj.54.2060.
- Zhang, Q.; Lin, D. & Bai, C. Motion state of fuel within shell in projection acceleration process. *Def. Sci. J.*, 2003, **53**, 259-265. doi: 10.14429/dsj.53.2274.
- Zhang, Q.; Wei K.Z.; Luo, A.M.; Wang D.G. & Qin B. Numerical simulation on dispersal character of fuel by central HE. *Def. Sci. J.*, 2007, **57** (4), 425-433. doi: 10.14429/dsj.57.1790.
- Singh, D.; Verma, P.C.; Vashisth, P.; Rawat, R.K.S. & Gupta, S.K. Laser proximity sensor for fuel-air explosive bomb. *Def. Sci. J.*, 2007, **57** (3), 167-172
- Apparao, A.; Rao, C.R. & Tewari, S.P. Studies on formation of unconfined detonable vapor cloud using explosive means. *J. Haz. Mat.*, 2013, **254-255**, 214-220. doi: 10.1016/j.jhazmat.2013.02.056.
- Apparao, A. & Rao, C.R. TNT equivalency of unconfined aerosols of propylene oxide. *Def. Sci. J.*, 2014, **64**, 431-437. doi: 10.14429/dsj.64.6851.
- Liu, L.J. & Zhang, Q. Comparison of detonation characteristics in energy output of gaseous JP-10 and propylene oxide in air. *Fuel*, 2018, **232**, 154-164. doi: 10.1016/j.fuel.2018.05.149.

11. Mixed Explosive Writing Group. Chemistry and echnology of high explosive. National Defence Industry Press, Beijing, China, 1983. pp.1-10 (Chinese).
12. Shi, C.J. & Ding, G. Anti-interference technology for fuze of twice-detonating FAE warhead. *J. Pro. Roc. Mis. & Guid.*, 2016, **36** (4), 51-54 (Chinese).
13. Bai C.H. & Zhang, Q. Detonation of fuel-air cloud. Chinese Science Press, Beijing, China, 2012. pp.137-145.
14. Xu, S.L.; Liu, J.C. & Liu R.H. Investigation on explosion of a fuel air explosive device. *J. Exp. Mech.*, 1995, **10** (3), 203-209 (Chinese).
15. Qin, M.;Wu, W.J. & Li, G.Q. Us special aviation bomb and its operational application. *O. I. Auto.*, 2007, 26 (1), 101 (Chinese).
doi: 10.3969/j.issn.1006-1576.2007.01.050
16. Zhang, X. Applied research of scientific visualization technology in FAE. Beijing Institute of Technology Beijing, China, 1996. (PhD Thesis)
17. Xu, Z.F. & Yu, J.B. Study on the influence of the number of initial detonation point of FAE to explosive power. *Tact. Miss. Tech.*, 2018, **191** (05), 108-111 (Chinese).
18. Pei, Y.X. Flight performance computation and simulation of mother-child FAE. Beijing Institute of Technology Beijing, China, 2002. (PhD Thesis)
doi: 10.3969/j.issn.1001-0645.2002.05.024
19. The Wring Group. Introduction of parachute technology. China National Defence Industry Press, Beijing, China, 1997, pp.34-120.
20. Hu, C.B.; Yang, Y.F.& Zhu S.R. Modeling and simulation of air-drop process With parachutes' twice inflating. *J. Air Force Radar Academy*, 2011, **25** (3), 209-212 (Chinese).
21. Yu, L. Aircraft rescue and personal protection technology. China National Defence Industry Press, Beijing, China, 2015. pp.25-67.
22. Xue, Z.; Li, S.; Xin, C.; Shi, L.P. & Wu, H.B. Modeling of the whole process of shock wave overpressure of free-field air explosion. *Def. Tech.*, 2019, **15**, 815-820.
doi: 10.1016/j.dt.2019.04.014.
23. Yang, X.; Yu, L.; Shi, X.L & Li, Y.L. Improved dynamic model on parachutes. *J. Nanjing. Uni. Aero. Astro.*, 2016, **48** (4), 481-485.
doi: 10.16356/j.1005-2615.2016.04.006.
24. Lou, H.F. Learning manual of MATLAB GUI. Edn 3rd. Beijing University of Aeronautics and Astronautics Press, Beijing, China, 2014, pp.1-189.

ACKNOWLEDGMENT

The authors wish to acknowledge the support of the National Science Foundation of China (11772057).

CONTRIBUTORS

Dr Qi Zhang obtained his PhD from the China University of Mining and Technology, Beijing. At present, he is working as Professor at the State Key Laboratory of Explosion Science and Technology, Beijing Institute of Technology. His research interests are in engineering blasting, and fuel-air explosive (FAE) and its applications. Contribution in the current study, he is the project leader in this current research group.

Mr Congliang Ye graduated from Nanjing University of Technology, in 2016. Now, he is doing his PhD at the Department of Mechanics Engineering of Beijing Institute of Technology. His research interest includes explosion blast, fuel-air explosive (FAE) and its applications. Contribution in the current study, he is responsible for modelling, simulation and analysis of the TDF trajectory.